

Interagency Monitoring of Protected Visual Environments (IMPROVE): Semiannual Quality Assurance Report

Air Quality Group | University of California, Davis | August 31, 2017

1. Introduction

The University of California Davis (UCD) Air Quality Group summarizes quality assurance (QA) parameters semiannually in this report as a contract deliverable for the Interagency Monitoring of Protected Visual Environments (IMPROVE) program (contract #P15PC00384). The primary purposes of this report are:

1. Provide the National Park Service (NPS) with graphical representations to illustrate key QA parameters for species measured within the network.
2. Identify and highlight observations of interest that may have short- or long-term impact on QA across the network or at particular sites.
3. Serve as a record and tool for ongoing UCD QA efforts.

The graphics shown in the main body of this report are a small subset of the many QA evaluations that UCD performs on a routine basis. They are selected to illustrate the nature and use of the QA tools, and provide a snapshot of the Network's internal consistency and recent trends. More finished analyses like those available in data advisories are outside the scope of this and subsequent reports, which are intended as a continuing series of timely performance overviews.

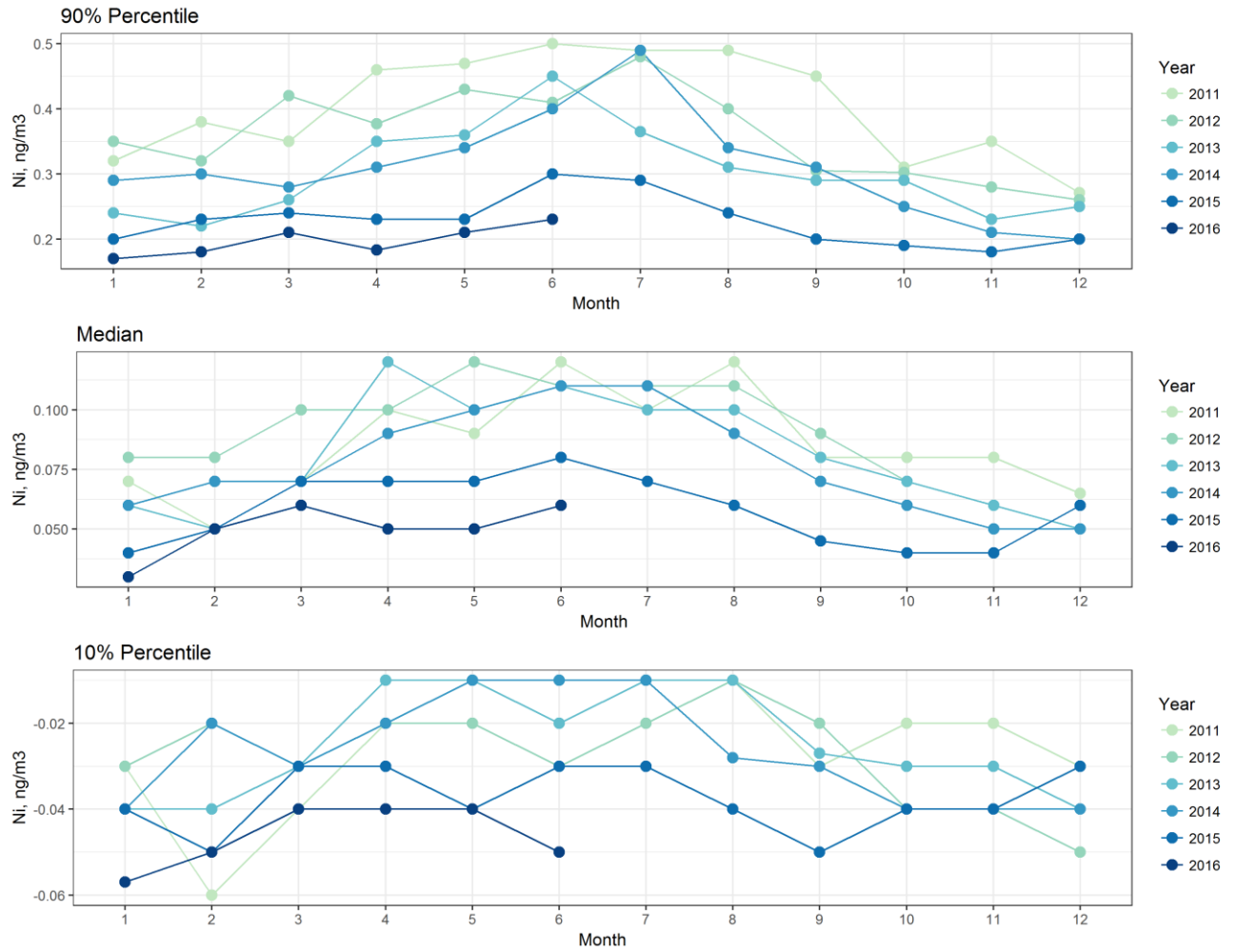
2. Network-wide QC plots

2.1 Multi-Year Time Series

These multi-year time series plots are used to examine large-scale trends or analytical problems. Shown in Figure 1 and Figure 2 are 90th percentile, median, and 10th percentile time series plots for nickel and vanadium concentrations (ng/m³), respectively. Five full years of network data (2011-2015) are shown to provide historical context for the first six months of the year currently under review (2016).

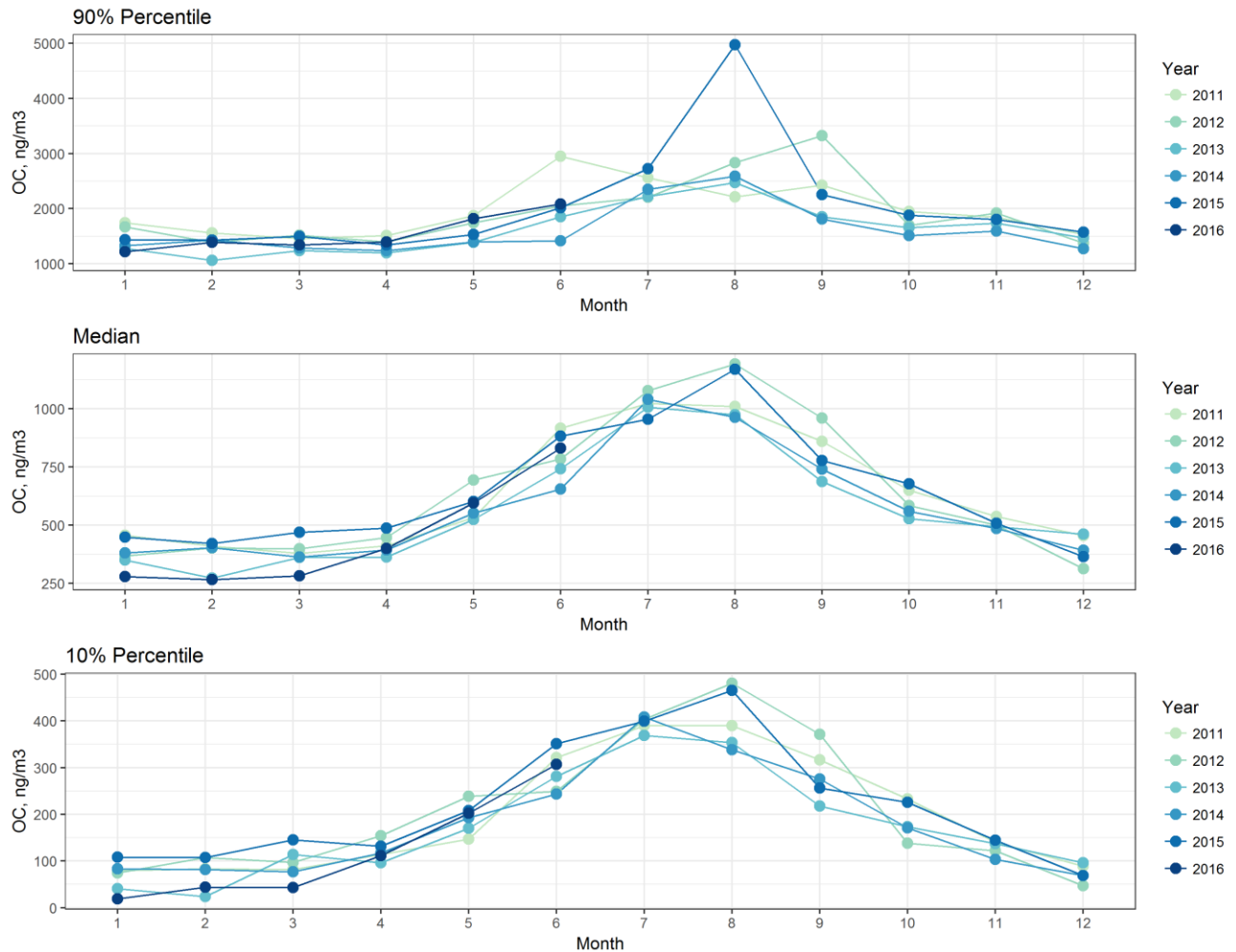
For 2015 and 2016, both nickel (Figure 1) and vanadium (Figure 2) concentrations are lower than previous years at the 90th percentile and median. This is particularly evident during the summer months and likely results from regulations on international shipping emissions implemented in January 2015.

Figure 1: Multi-year time series, nickel (Ni).



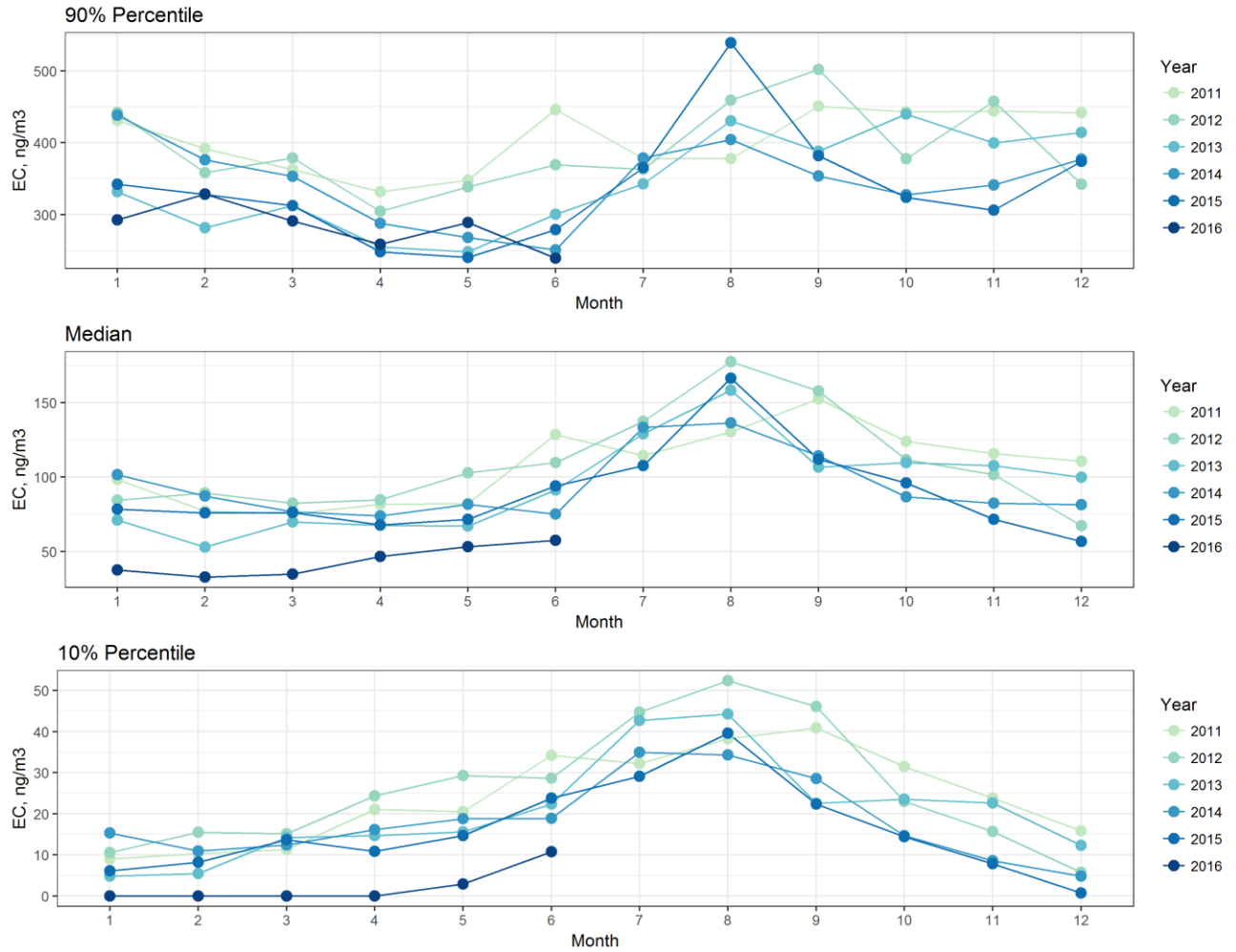
Starting in January 2016, Desert Research Institute (DRI) performed carbon analysis using DRI Model 2015 Multiwavelength Thermal/Optical Carbon Analyzers, whereas from 2005 through 2015 the older DRI Model 2001 analyzers were used. Shown in Figure 3 and Figure 4 are organic carbon (OC) and elemental carbon (EC) network-wide percentile plots, respectively.

Figure 3: Multi-year time series, organic carbon (OC).



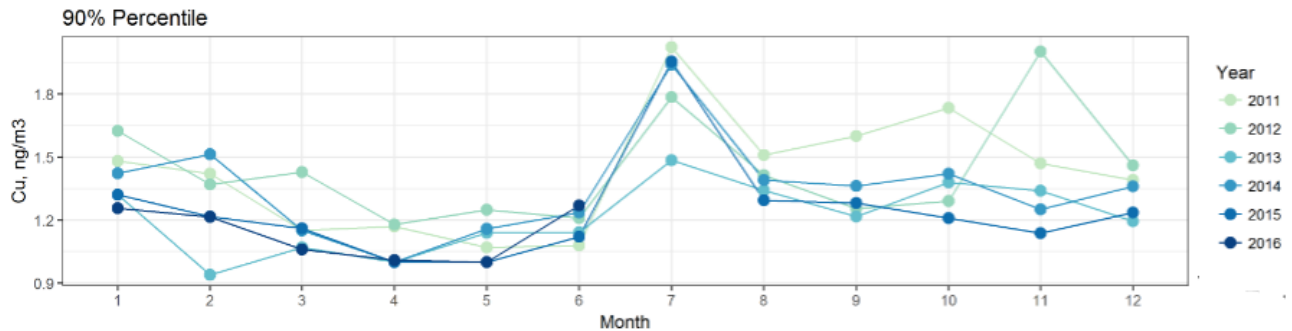
Early 2016 (January through June) EC concentrations are noticeably lower than the previous five years.

Figure 4: Multi-year time series, elemental carbon (EC).



Enhanced concentrations of copper (Cu) during July at the 90th percentile are observed during all years (Figure 5). Copper compounds are employed to produce blue coloration in fireworks, and the elevated July Cu concentrations are likely associated with Independence Day celebrations.

Figure 5: Multi-year time series, copper (Cu).



2.2 Cross-module comparisons

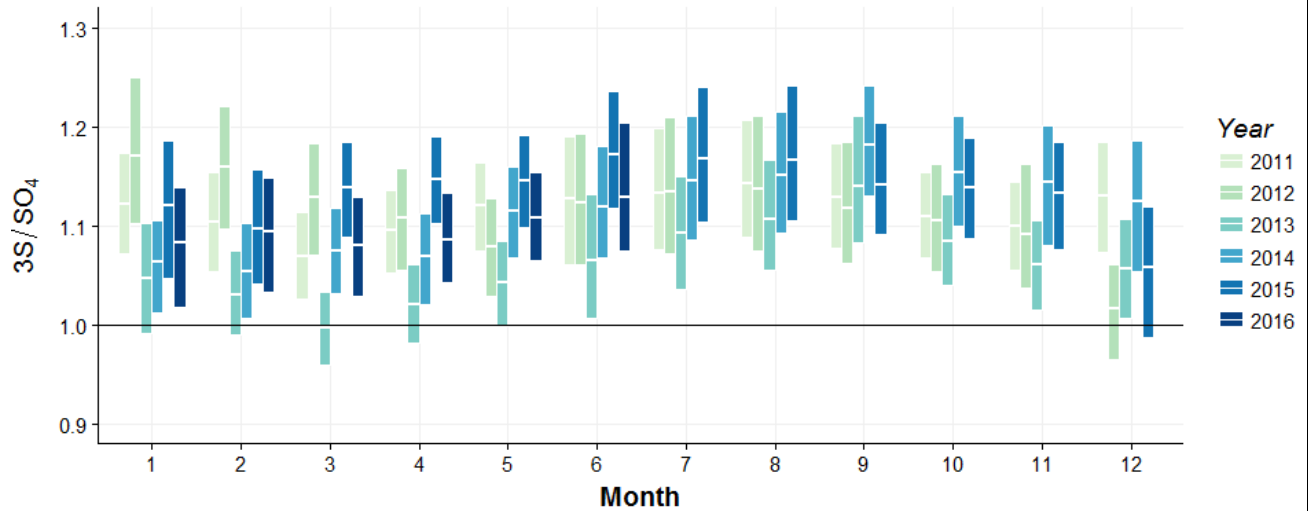
The following graphs compare two independent measures of aerosol properties that are expected to correlate and are used to identify analytical or sampling issues. The IMPROVE sampler has four sampling modules:

- Module-A: Collection of fine particles with aerodynamic diameter less than 2.5 μm ($\text{PM}_{2.5}$) on polytetrafluoroethylene (PTFE) filters for gravimetric, x-ray fluorescence (XRF), and optical absorption by hybrid integrating plate/sphere (HIPS) analysis.
- Module-B: Collection of $\text{PM}_{2.5}$ on nylon filters for ion chromatography (IC) analysis.
- Module-C: Collection of $\text{PM}_{2.5}$ on quartz filters for thermal optical analysis (TOA).
- Module-D: Collection of particles with aerodynamic diameter less than 10 μm (PM_{10}) on PTFE filters for gravimetric analysis.

2.2.1 Sulfur vs. Sulfate

Filters collected from the A-Module are analyzed for elemental sulfur using XRF, and filters collected from the B-Module are analyzed for sulfate (SO_4) using IC. The molecular weight of SO_4 (96 g/mol) is three times the atomic weight of S (32 g/mol), so the concentration ratio $(3 \times \text{S})/\text{SO}_4$ should be one if all particulate sulfur is present as water-soluble sulfate. In practice, real measurements routinely yield a ratio greater than one (Figure 6), suggesting the presence of some sulfur in a non-water soluble form of sulfate or in a chemical compound other than sulfate.

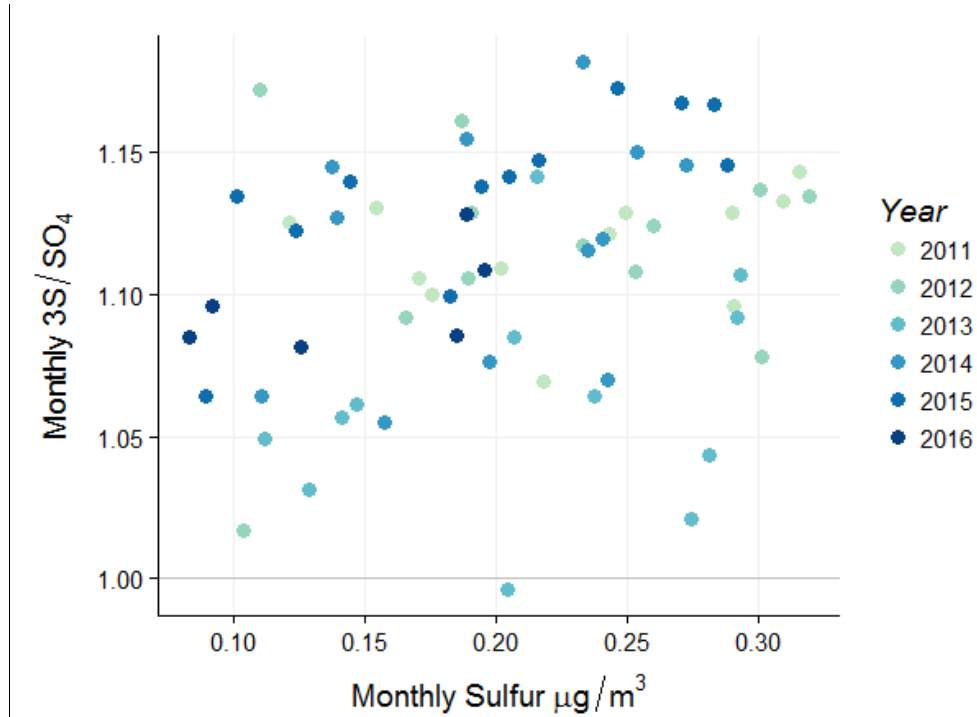
Figure 6: Multi-year time series of $(3 \times \text{S})/\text{SO}_4$.



The 2013 $(3 \times \text{S})/\text{SO}_4$ ratio is lower than earlier and later years, with a median value dropping below one in March 2013; we are not aware of analytical or sampling changes that explain the low ratios in 2013.

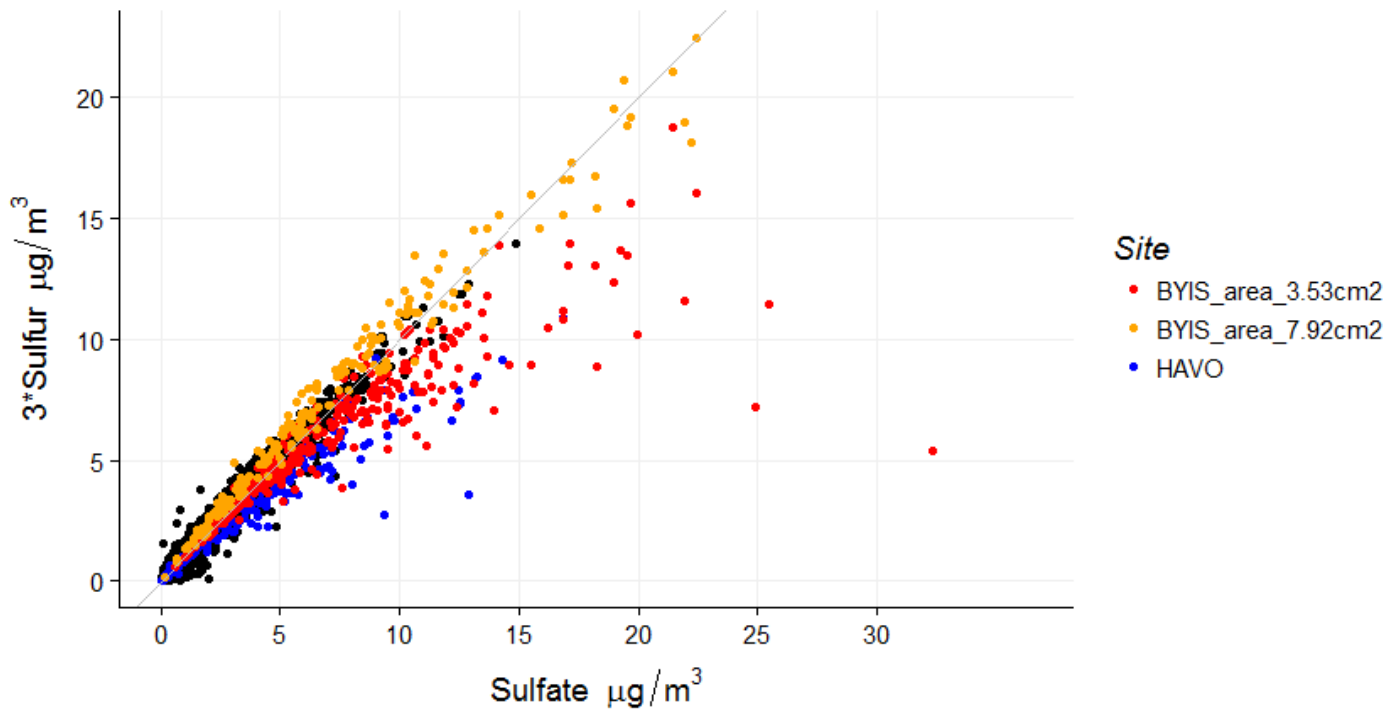
As seen in Figure 6, there is seasonal variability in the $(3\times S)/SO_4$ ratio with higher ratios observed in the late summer and early fall. Such a seasonal pattern might conceivably arise from an additive offset in one or the other of the measurements, such as produced by an over- or under-correction for the Nylon filter blank: since both species are strongly seasonal, a constant concentration offset in one and not the other would produce a seasonal bias in their ratio. Figure 7, a multi-year scatter plot of the $(3\times S)/SO_4$ ratio as a function of the sulfur concentration, discounts this potential mechanism as an important source of the observed seasonality, showing the $(3\times S)/SO_4$ ratio variability to be largely independent of concentration. It is interesting to note that the 2013 outliers are less visually evident in this scatter plot than they are in the Figure 6 box plot.

Figure 7: Multi-year scatter plot of $(3\times S)/SO_4$ versus sulfur.



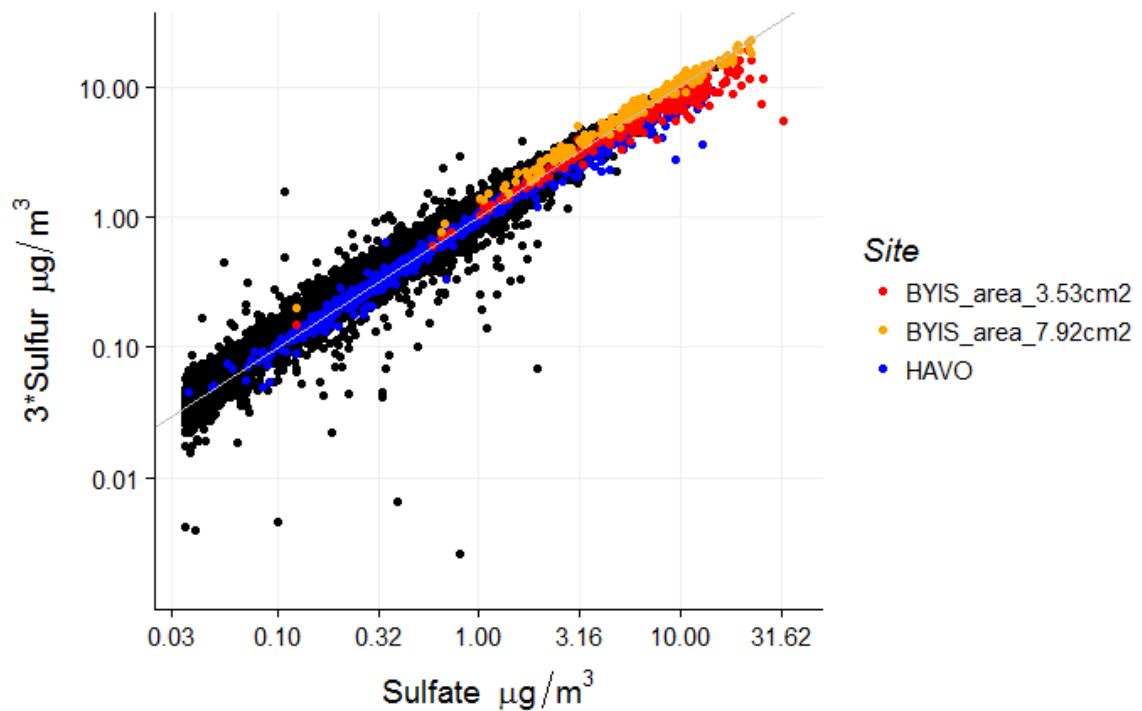
The BYIS1 (South Korea), BYISX (South Korea, collocated), and HAVO1 (Hawaii Volcanoes National Park) sites show deviation of the $(3\times S)/SO_4$ ratio, compared to other sites in the network (Figure 8). The $(3\times S)/SO_4$ ratios at these sites are lower than typically observed, with $(3\times S)/SO_4$ becoming further depressed at higher concentrations. At HAVO1, this behavior may be due to sampling artifacts on the Nylon filter from volcanic source gases. Analogous sampling artifacts associated with the high concentrations downwind of China may contribute to the similar behavior observed in South Korea.

Figure 8: Comparison of $3\times S$ with SO_4 at BYIS1 (South Korea), BYISX (South Korea, collocated with larger sample filter), and HAVO1 (Hawaii Volcanoes National Park), 2011 through 2015. All other network data from these years are plotted in black.



To highlight the importance of evaluating data from multiple views, we also include a comparison of the $(3 \times S)/SO_4$ ratio for these sites on a logarithmic scale (Figure 9). While the BYIS1, BYISX, and HAVO1 deviations are clear in Figure 8, they are less apparent when viewed logarithmically.

Figure 9: Logarithmic comparison of $3 \times S$ with SO_4 at BYIS1 (South Korea), BYISX (South Korea, collocated with larger sample filter), and HAVO1 (Hawaii Volcanoes National Park), 2011 through 2015. All other network data from these years are plotted in black.



2.2.2 PM_{2.5} vs. Reconstructed Mass (RCMN)

Filters from the A-Module are analyzed gravimetrically (i.e., weighed before and after sample collection) to determine PM_{2.5} mass. Gravimetric data can be compared to reconstructed mass (RCMN), where the RCMN composite variable is derived from chemical measurements. The formulas used to estimate the mass contributions from various chemical species are taken from UCD IMPROVE SOP 351, Data Processing and Validation, where their derivations and underlying assumptions are explained. In the simple case where valid measurements above detection limits are available for all needed variables, reconstructed mass is the following sum:

$$\text{RCMN} = (4.125 \times \text{S}) + (1.29 \times \text{NO}_3^-) + (1.8 \times \text{OC}) + (\text{EC}) + \\ (2.2 \times \text{Al} + 2.49 \times \text{Si} + 1.63 \times \text{Ca} + 2.42 \times \text{Fe} + 1.94 \times \text{Ti}) + (1.8 \times \text{Cl})$$

The parenthesized components represent the mass contributions from, in order, ammonium sulfate, ammonium nitrate, organic compounds, elemental carbon, soil, and sea salt.

The RCMN reported here uses chlorine for the sea salt component, which differs from the reconstructed fine mass (RCFM) calculated by CIRA. RCMN and RCFM are the same composite variable (with different names), except RCFM uses chloride instead of chlorine for the sea salt component. Future reports will use chloride for the RCMN calculation to be in alignment with CIRA.

The RCMN/PM_{2.5} ratio exhibits seasonal variability, with the lowest ratios during the summer months (Figure 10). Relative to previous years, early 2016 (January through June) ratios are notably lower. Low RCMN/PM_{2.5} ratios can result from inclusion of unbound water in the gravimetric PM_{2.5} measurement and/or loss to volatilization of ammonium nitrate from the A-module PTFE filters before weighing, among other causes. Lower-than-expected 2016 elemental carbon values, shown in Section 2.1, could contribute to the depressed RCMN. Figure 11 shows that the ratio of RCMN to PM_{2.5} decreases with increasing PM_{2.5} concentrations.

Figure 10: Multi-year time series of RCMN/PM2.5.

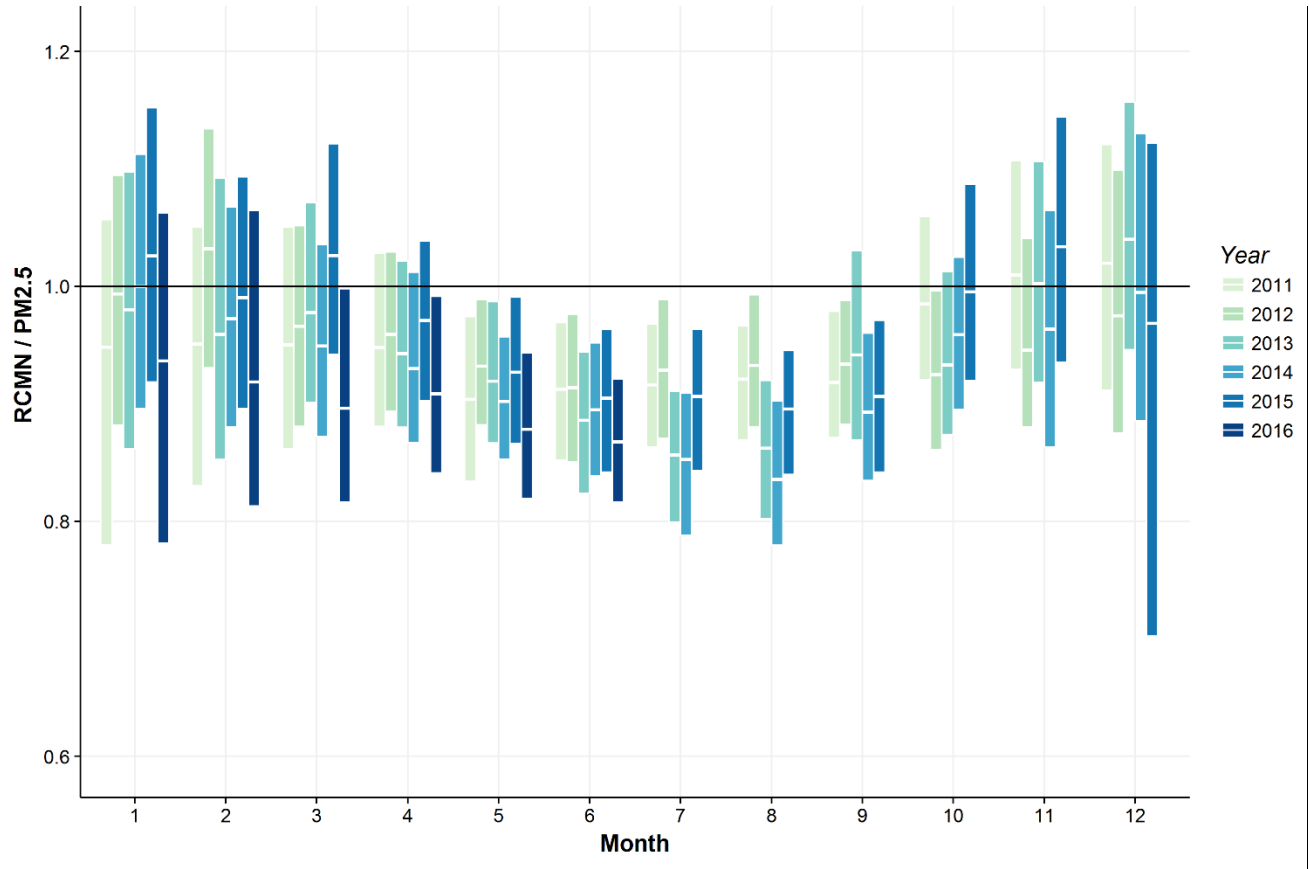
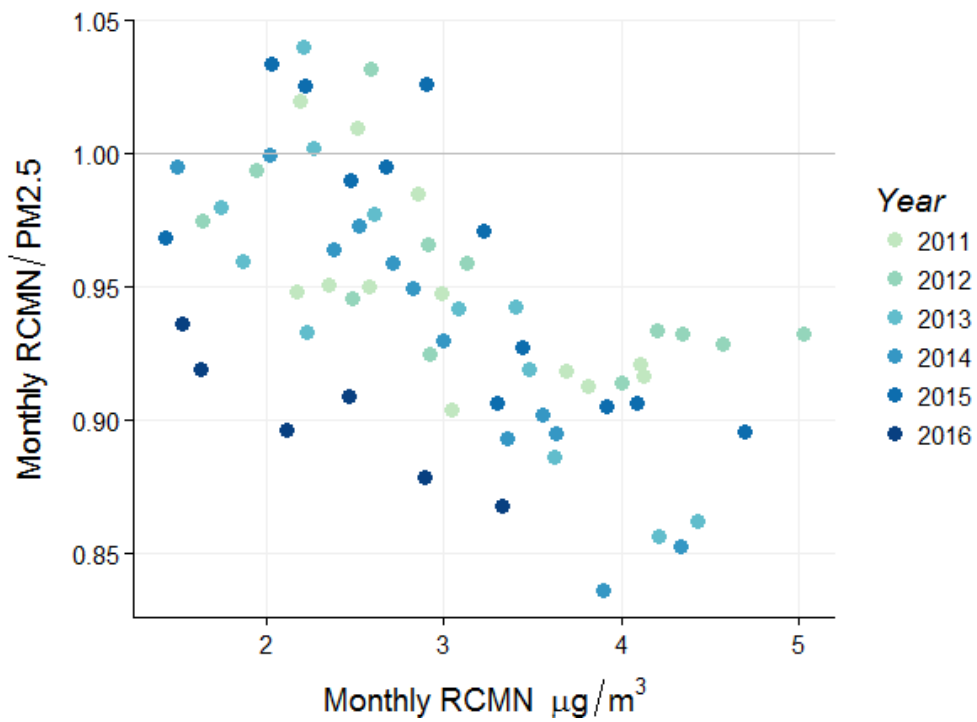


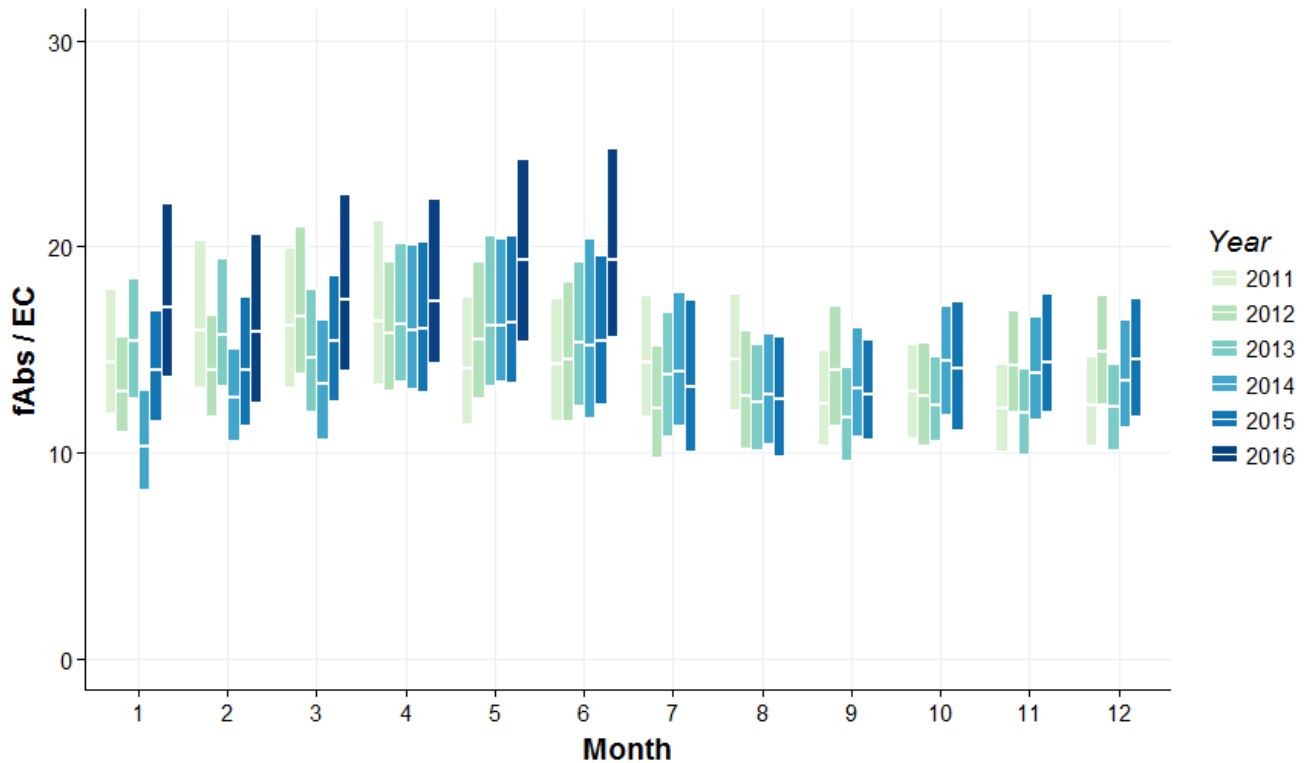
Figure 11: Multi-year scatter plot of RCMN/PM2.5 relative to RCMN.



2.2.3 Optical absorption vs. elemental carbon

The hybrid integrating plate/sphere (HIPS) instrument measures optical absorption, allowing for calculation of absorption coefficients (Fabs, where units are Mm^{-1}) from A-Module PTFE filters. Absorption coefficients are expected to correlate with C-Module elemental carbon (EC, where units are $\mu\text{g}/\text{m}^3$) measured by thermal optical reflectance (TOR). The Fabs/EC ratio (with units m^2/g) exhibits seasonal variability with lower ratios during the summer months, corresponding with higher concentrations of EC (Figure 12).

Figure 12: Multi-year time series of Fabs/EC, where Fabs is in Mm^{-1} and EC is in $\mu\text{g}/\text{m}^3$.



Higher Fabs/EC ratios are observed in early 2016 (January through June), corresponding with lower EC concentrations (Figure 4). This shift in the ratio coincides with the change in instrumentation discussed in Section 2.1.

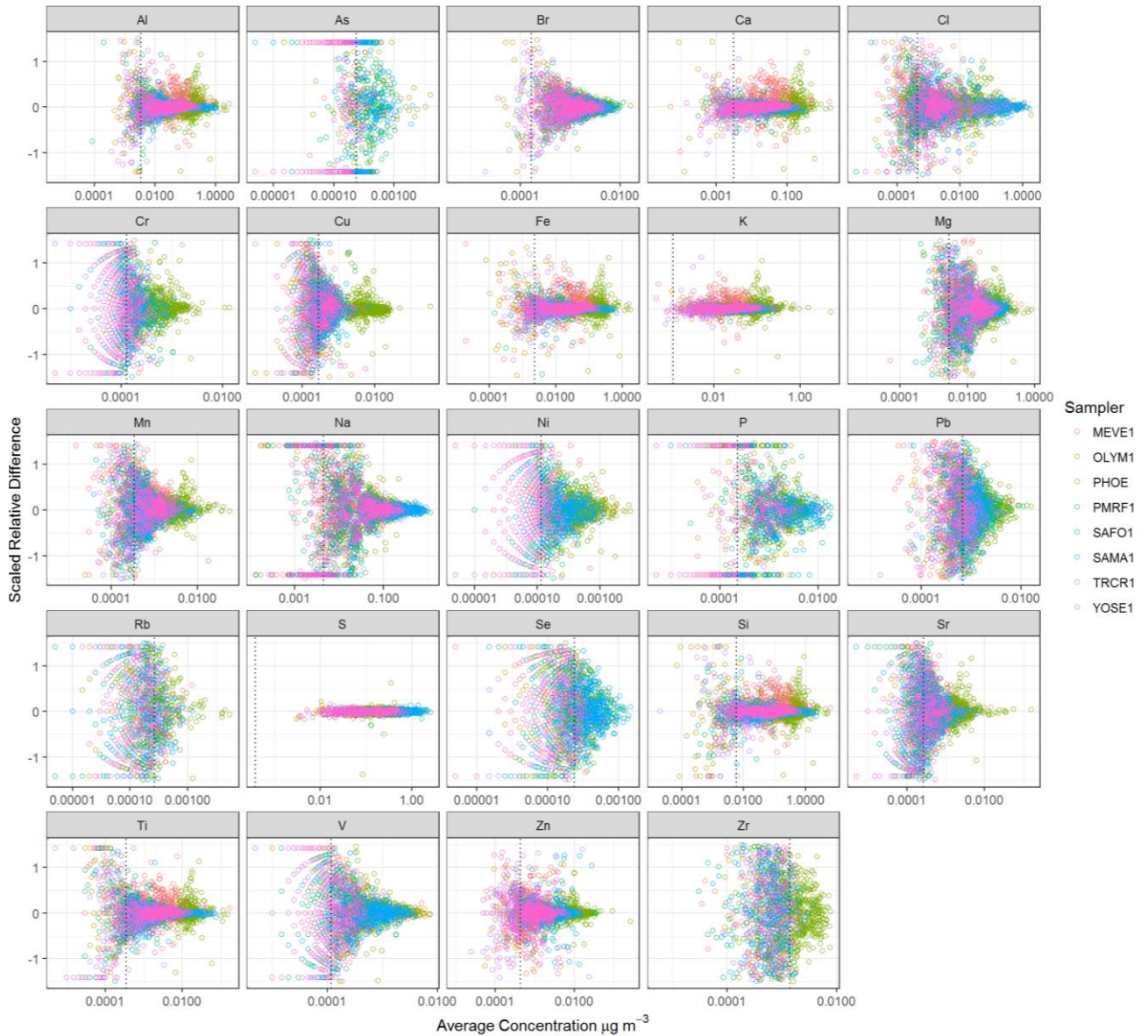
2.3 Collocated Data Plots

There are several sites across the IMPROVE network with collocated modules, where samples are collected and analyzed using identical analytical systems. Measurements from collocated samplers can be compared using scaled relative difference,

$$\textit{Scaled Relative Difference} = \frac{(\textit{collocated} - \textit{routine}) / \sqrt{2}}{(\textit{collocated} + \textit{routine}) / 2}$$

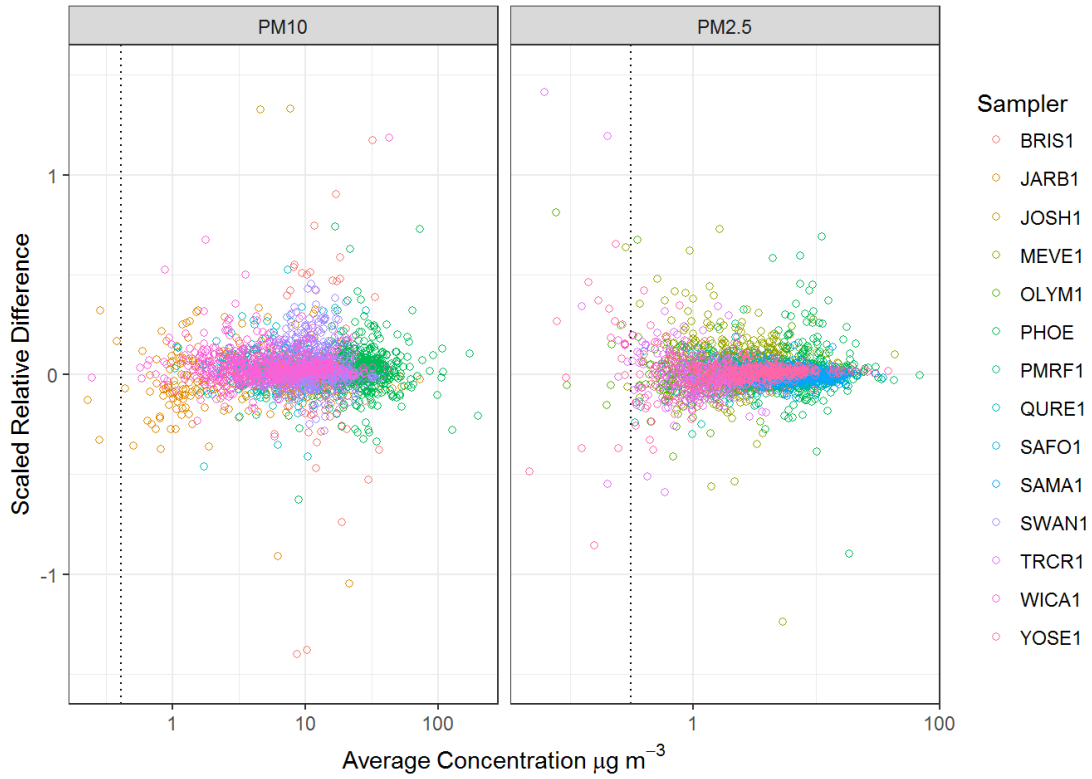
Scaled relative difference allows for direct comparison of measurements across a range of concentrations, taking into account that actual difference at high concentration will likely be greater than at low concentration. The scaled relative differences are expected to be high at concentrations close to the detection limit, decrease with increasing concentration, and stabilize when the concentration is well above the detection limit (Figure 13).

Figure 13: Scaled relative difference for element measurements at sites with collocated modules across the IMPROVE network (2011-2016). Dotted vertical lines indicate the detection limits.



Scaled relative difference for PM_{2.5} exhibits a similar trend with greater relative difference at lower concentration (Figure 14). For PM₁₀ the relative difference is comparable across the concentration range because the concentrations are well above the detection limit (Figure 14).

Figure 14: Scaled relative difference for PM10 and PM2.5 at 14 collocated sites across the IMPROVE network (2011-2016).



As discussed in UCD IMPROVE SOP 351, Data Processing and Validation, fractional uncertainty is calculated for each species using data from collocated sites. Current fractional uncertainties are calculated using 2005-2013 data (Table 1). Beginning with the next IMPROVE QA report (anticipated delivery, January 31, 2018), fractional uncertainty calculations will be updated annually.

Table 1: Fractional uncertainty, 2005-2013.

Species (Ions)	Fractional Uncertainty	Species (Carbon)	Fractional Uncertainty	Species (Elements)	Fractional Uncertainty
Chloride	0.08	Organic Carbon (1)	0.23	Na	0.14
Nitrite	0.22	Organic Carbon (2)	0.15	Mg	0.15
Nitrate	0.04	Organic Carbon (3)	0.13	Al	0.09
Sulfate	0.02	Organic Carbon (4)	0.15	Si	0.10
Ammonium	0.02	Organic Pyrolyzed (TR)	0.13	P	0.25
Sulfur Dioxide	0.04	Elemental Carbon (1)	0.10	S	0.03
		Elemental Carbon (2)	0.17	Cl	0.14
		Elemental Carbon (3)	0.42	K	0.03
				Ca	0.06
				Ti	0.11
				V	0.12
				Cr	0.22
				Mn	0.13
				Fe	0.06
				Ni	0.16
				Cu	0.12
				Zn	0.06
				As	0.25
				Se	0.25
				Br	0.10
				Rb	0.25
				Sr	0.16
				Zr	0.25
				Pb	0.13

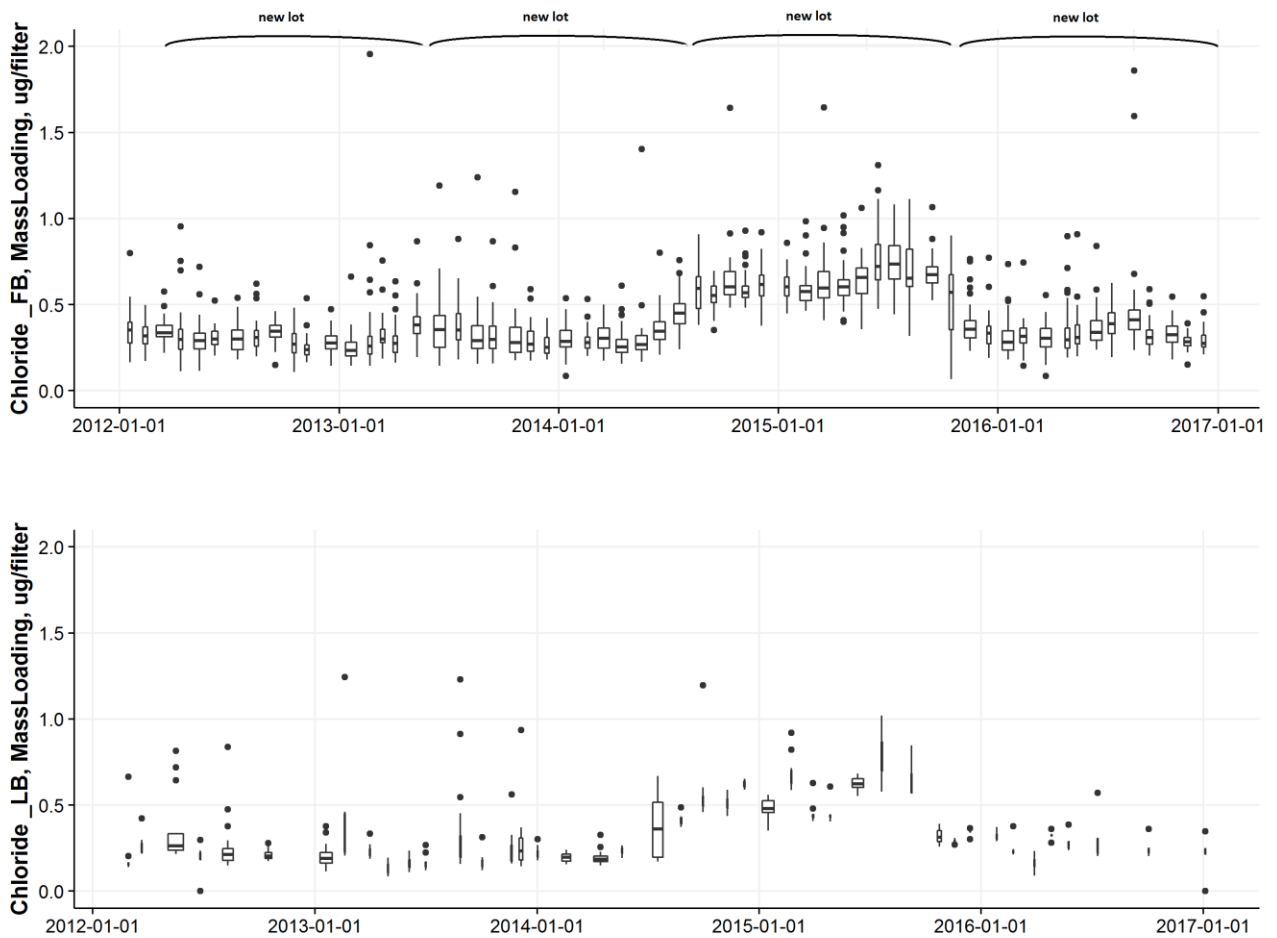
3. Analytical QC Checks

Field blanks are an integral part of the QC process and are collected at sampling sites across the network by exposing filters to the same conditions and handling that a sampled filter experiences but without pulling air through the filter. Field blanks are analyzed using the same process as sampled filters and results allow for artifact correction as part of the concentration calculation. Artifacts result from contamination in the filter material or in handling and analysis.

3.1 Ions

Nylon filters are received from the manufacturer in lots that typically last one year. Acceptance criteria are established to evaluate background concentrations on each new lot of filters, however, there can be substantial variability in ion species across different lots. Analysis of field and lab blanks are an important tool for artifact evaluation and correction. Figure 15 illustrates the variability of chloride across lots, as seen for both field and lab blanks. Transition to new lots occurs over a period of weeks; thus the shift in field blank concentrations gradually manifest over time rather than abruptly.

Figure 15: Time series of chloride measured on nylon filter field (FB) and lab (LB) blanks.



3.2 Carbon

Quartz filters are pre-fired by DRI. Quartz filter field blanks exhibit low concentrations of EC, typically below $0.5 \mu\text{g}/\text{m}^3$, with no seasonal pattern (Figure 16). Conversely, higher field blank concentrations are observed for OC, with the highest values during summer months often over $5 \mu\text{g}/\text{m}^3$ (Figure 17).

Figure 16: Time series of elemental carbon artifact on quartz filter field blanks.

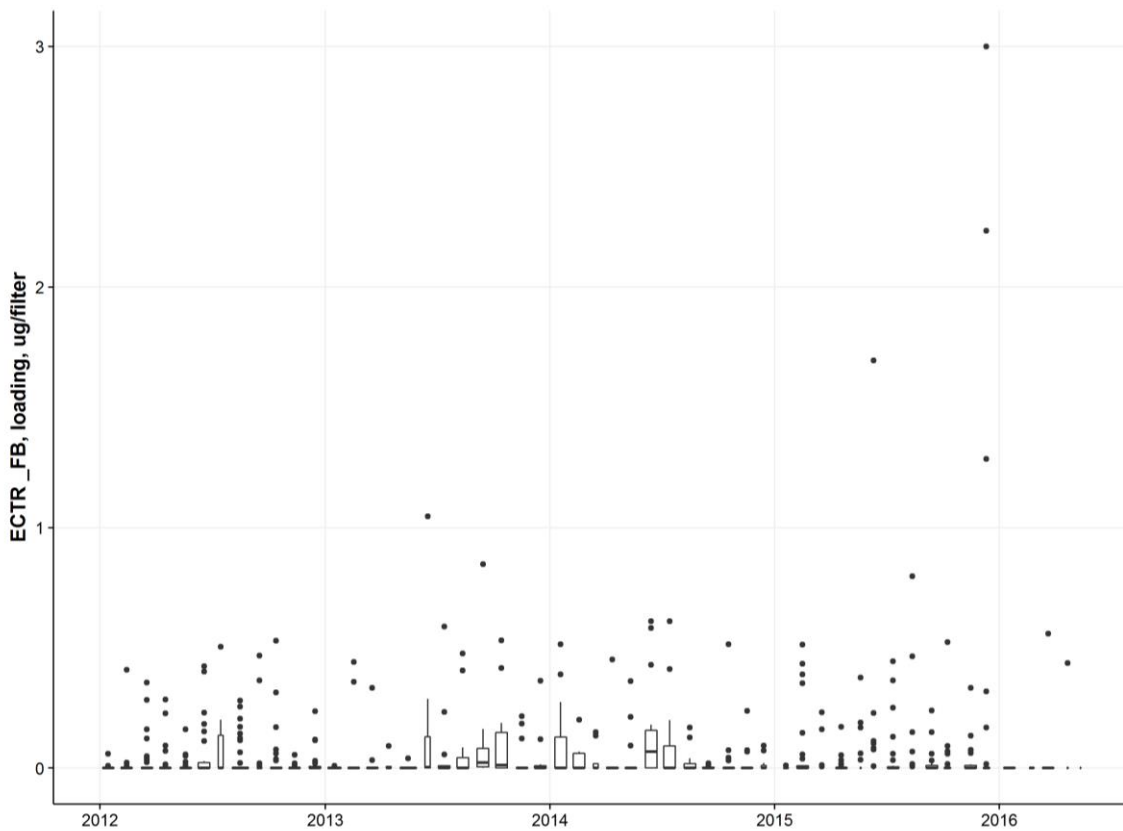
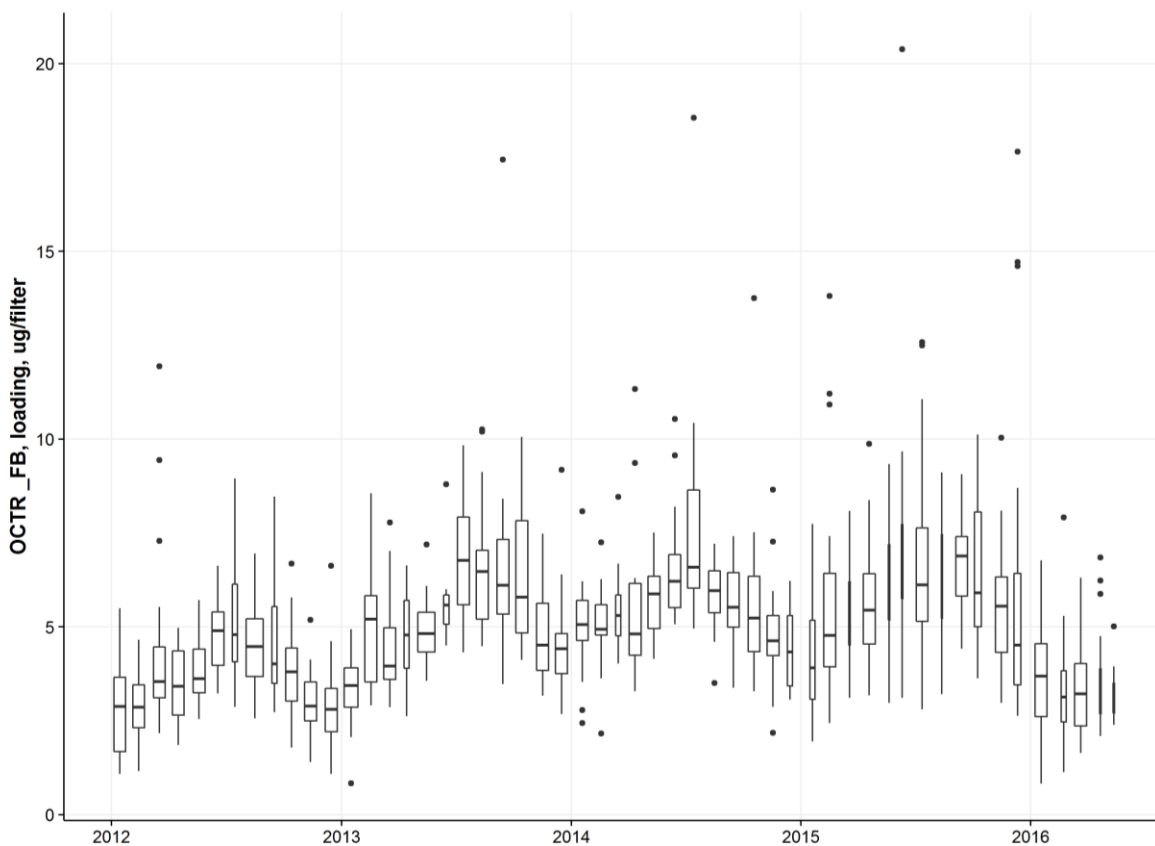


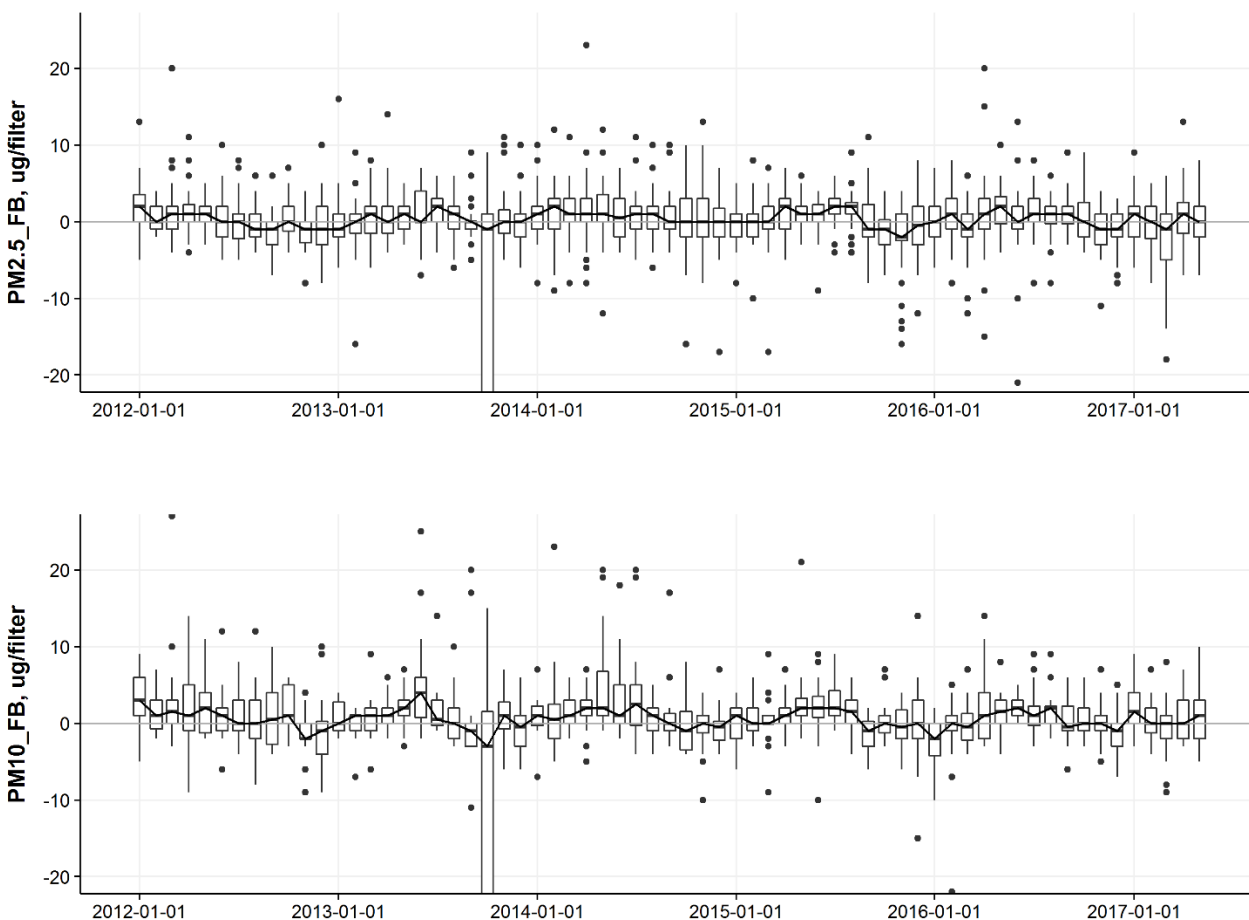
Figure 17: Time series of organic carbon artifact on quartz filter field blanks.



3.3 Mass

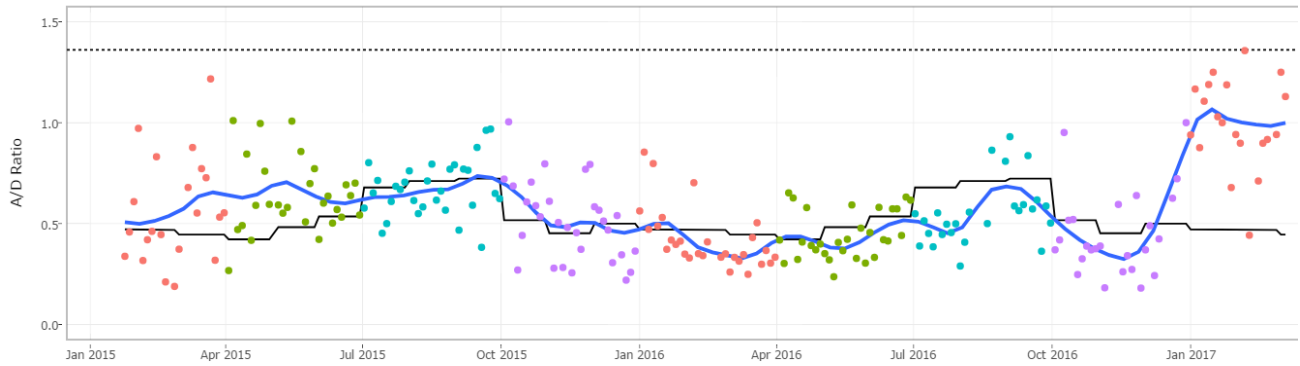
PTFE filter field blanks from the A-module (fine particles, $PM_{2.5}$) and D-module (course particles, PM_{10}) are gravimetrically analyzed to monitor contamination levels and balance stability (Figure 18). The distributions span zero, but exhibit slight seasonality with more positive values in the summer.

Figure 18: Time series of PM_{2.5} and PM₁₀ on PTFE filter field blanks.



As part of the gravimetric laboratory quality control, the ratio of PM_{2.5} A-Module mass over PM₁₀ D-Module mass – smoothed using a locally-weighted average (LOESS) – is compared to the multi-year monthly mean (Figure 19). The LOESS regression (blue line) is expected to closely follow the historical monthly mean (black line). UCD laboratory staff successfully used this tool to identify a problem at the Guadalupe Mountains site (GUMO1) when the LOESS regression dramatically increased to roughly twice the historical monthly mean (Figure 19). Through troubleshooting with the operator, UCD determined that the A/D ratio disruption was the result of a missing D-Module inlet. The site ultimately had too many samples invalidated and failed to meet the Regional Haze Rule completeness criteria. However, this serves as an example where the UCD data validation interface was a valuable tool for catching an obscure field problem and prevented additional samples from being lost.

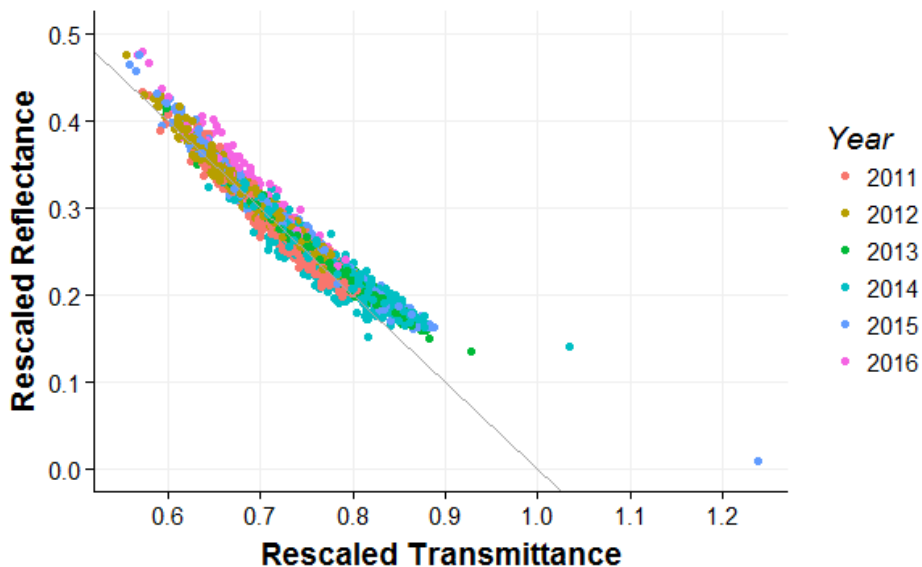
Figure 19: Screenshot example of UCD data validation interface used by laboratory staff. Ratio of PM_{2.5} mass (A) over PM₁₀ mass (D) at the Guadalupe Mountain site (GUMO), represented as raw measurements not adjusted for flow rates. Points are individual sample days (pink = Q1, green = Q2, blue = Q3, purple = Q4). Black line is the multi-year monthly mean. Blue line is the locally weighted average (LOESS).



3.4 Optical Absorption

Optical absorption measurements on PTFE filters are performed using the Hybrid Integrating Plate/Sphere (HIPS) instrument. As part of HIPS quality control, field blanks are analyzed and evaluated with the expectation that calibrated reflectance and transmittance will relate as $R_{cal} = 1 - T_{cal}$ (solid line, Figure 20).

Figure 20: Reflectance versus transmittance as measured by HIPS, where values are rescaled per calibration.



4 Documentation

Current standard operations procedures (SOPs) are available at:

<http://airquality.crocker.ucdavis.edu/improve/standard-operating-procedures-sop/>

Table 2: Summary of upcoming project documentation deliverables.

Deliverable	Upcoming Delivery Date
SOPs and TI documents	November 30, 2017
Quarterly Site Status Report	November 15, 2017 (Q3) February 15, 2017 (Q4)
Semiannual Quality Assurance Report	January 31, 2018

5 Site Maintenance Summary

5.4 Summary of Repair Items Sent

UCD maintains and repairs the samplers at each IMPROVE site. The UCD Field Group works closely with site operators to address maintenance and repair issues to ensure continuous operation and sample collection at the sites. UCD maintains an inventory of sampler components for shipment to the sites on short notice. Table 3 summarizes the equipment shipped in the last six months (January through June, 2017) to repair samplers. The number of controllers replaced (36) is a major concern and is related to the age of the equipment. UCD has developed and is currently field-testing new sampler controllers. In the first six months of 2017 UCD installed four new controllers in the field: PHOE, FRES, OWVL, and ROMO.

Table 3: Repair items shipped to IMPROVE sites, 1/1/2017 through 6/30/2017.

Item	Quantity	Sites
Controller	36	ZICA, BIRM, PACK, MAKA, LABE, NOAB, HOOV, PORE, LOND, SHRO, LTCC, STIL, FLAT, GAMO, SAGU, NOCA, CAPI, IKBA, THBA, SULA, MEVE, VIIS, SYCA, CACR, UPBU, LASU, BRIS
Pump	48	GLAC, NOCA, WICA, ORPI, KALM, NOGA, REDW, PACK, ACAD, SAWT, NOCA, AGTI, ZICA, WEMI, VIIS, GRSA, BALD, BRIS, PITT, CHIR, BOWA, CACO, RAFA, KPBO, BAND, SAMA, DOME, VILA, PRIS, THSI, BRCA, HAVO, BRIS, HOOV
Electronic boxes	19	LYEB, SAWT, CANY, SHRO, REDW, MONT, BRIS, STIL, EGBE, CANY, MEVE, CACR, NOCA, LASU
Module Cable	9	SAWT, CRMO, PEFO, SHRO, BOND, BRIS, NOCA, LASU
Relay Box	9	ISLE, OKEF, SAWT, VIIS, STIL, PENO, HOOV
Sierra PM ₁₀ Inlet	3	BRIS, GUMO, VIIS
PM _{2.5} Inlet Cap	2	SULA, BRIS
Flow Check Kits	8	NEBR, NOCA, LAVO, VIIS, BIBE, BOAP, GRCA, LABE
Module	3	KPBO, SAWT, NOCA

5.5 Summary of Site Visits

The UCD Field Group visits IMPROVE network sites biennially to provide routine maintenance and cleaning. Sites are occasionally visited more frequently to address emergency issues. Table 4 summarizes the visits that UCD performed January through June, 2017.

Table 4: UC Davis field visits to IMPROVE sites, 1/1/2017 through 6/30/2017.

Site Name	Date Visited	Notable / Unusual Repair Notes	Improvements Requested
SWAN	2/26/2017	Repaired D motor connector. Replaced D critical orifice.	
ROMA	2/28/2017	Redistributed plugs to better balance load.	
OKEF	3/2/2017	Changed weather stripping, temp probe, and keypad.	Site is on one 20A circuit; char marks on one of the outlets.
SAMA	3/3/2017	Site was on a triple tap extension cord that melted. Eliminated cord and utilized second outlet already on site.	
CHAS	3/4/2017	Moved location of an outlet to eliminate an unneeded extension cord.	
EVER	3/6/2017	Added support lumber to prolong life of stand. Replaced broken electrical conduit.	Major structural problems from rot; needs full rebuild.
PHOE5	3/26/2017	New controller flow check.	
PHOE1	3/26/2017		
ORPI	3/27/2017		
SAGU	3/28/2017		
SAWE	3/29/2017		
NOGA	3/30/2017		
CHIR	3/31/2017		
TONT	4/1/2017		
MING	4/25/2017	Changed critical orifice for more consistent ORI readings.	Site is on one 20A circuit
MACA	4/27/2017	Cleared spider web from D stack.	
COHU	4/28/2017		
LIGO	4/29/2017		
SHRO	4/30/2017		Site is on one 20A circuit
GRSM	5/1/2017	Changed ebox, controller, and two pumps.	Site is on one 20A circuit
SIPS	5/2/2017		Relays on a triple tap; site needs a four-outlet receptacle with two 20A circuits.
BIRM	5/3/2017		Site located close to edge of deck; needs to be moved inward.
ATLA	5/4/2017		
SAGA	5/23/2017	Major damage cleanup from shed flipping; anchor and guy-wires added. All equipment replaced.	
TRIN	6/2/2017	Site maintenance after long shutdown.	
JARI	6/6/2017	Cleared spider web from D funnel.	Site is on one 20A circuit.

SHEN	6/7/2017		Site is on one 20A circuit.
DOSO	6/8/2017	Replaced D stack o-ring.	
FRRE	6/10/2017	Replaced B ebox to fix ORI.	
QUCI	6/10/2017	Major stand rebuild; two full days spent building new pump enclosure and flooring.	Site had mice and wasps.
PITT	6/12/2017		
EGBE	6/13/2017	Leaky C module; cyclone replaced.	Site appears to be on one 15A circuit. Controller plug/outlet not protected from weather.
DETR	6/14/2017	C pump replaced.	
WHPE	6/19/2017	Broken Sierra PM ₁₀ inlet jar on arrival.	
SHMI	6/20/2017	Ebox replacement.	Power may be cutting off regularly. Requested monitoring with voltage quality recorder.
GRSA	6/21/2017	C stack found raised on arrival.	
ROMO	6/22/2017	New controller installed.	
FLTO	6/24/2017		
WHRI	6/25/2017	Controller replacement.	
CANY	6/26/2017		
CAPI	6/28/2017		
BRCA	6/30/2017	B manifold replaced.	